

Constraining the dark energy models using Baryon Acoustic Oscillations: An approach independent of $H_0 \cdot r_d$

Denitsa Staicova¹ and David Benisty^{2,3}

¹ Institute for Nuclear Research and Nuclear Energy, Bulgarian Academy of Sciences, Sofia, Bulgaria

² DAMTP, Centre for Mathematical Sciences, University of Cambridge, Wilberforce Road, Cambridge CB3 0WA, UK

³ Kavli Institute of Cosmology (KICC), University of Cambridge, Madingley Road, Cambridge, CB3 0HA, UK

ABSTRACT

The H_0 tension and the accompanying r_d tension are a hot topic in current cosmology. In order to remove the degeneracy between the Hubble parameter H_0 and the sound horizon scale r_d from the Baryon Acoustic Oscillations (BAO) datasets, we redefine the likelihood by marginalizing over the $H_0 \cdot r_d$ parameter and then we perform full Bayesian analysis for different models of dark energy (DE). We find that our uncalibrated by early or late physics datasets cannot constrain the DE models properly without further assumptions. By adding the type IA supernova dataset, the models are constrained better with smaller errors on the DE parameters. The two BAO datasets we use – one with angular measurements and one with angular and radial ones with their covariances, show statistical preferences for different models, with Λ CDM being the best model for one of them. Adding the Pantheon SnIA dataset with its covariance matrix boosts the statistical preference for Λ CDM.

Key words. Baryon Acoustic Oscillations, Dark Energy, Dark Matter, Large Scale Structure, Hubble Tension

1. Introduction

A turning point in modern cosmology is the measurement of the Hubble constant H_0 revealing the current accelerated expansion of the Universe Riess et al. (1998); Freedman & Madore (2010). Estimation of H_0 from the late Universe can be obtained from direct measurements such as distance ladders, strong lensing, gravitational wave standard sirens etc. Freedman et al. (2001); Perlmutter et al. (1999); Riess et al. (2016, 2021). The latest SH0ES measurement based on the Supernovae calibrated by Cepheids is $H_0 = 73.04 \pm 1.04 \text{ km s}^{-1} \text{ Mpc}^{-1}$ at 68% CL Riess et al. (2022b). Further improvement comes from a SH0ES measurement of distance ladder calibrated by parallaxes of Cepheids in open clusters, which combined with all anchors, yields $H_0 = 73.01 \pm 0.99 \text{ km s}^{-1} \text{ Mpc}^{-1}$ Riess et al. (2022a).

Another type of measurement is provided by the Planck collaboration which uses temperature and polarization anisotropies in the Cosmic Microwave Background (CMB) to obtain $H_0 = 67.27 \pm 0.6 \text{ km s}^{-1} \text{ Mpc}^{-1}$. The discrepancy between local model-independent measurements of H_0 and the early-Universe CMB values can reach 5.3σ and it is one of the fundamental problems in cosmology Schöneberg et al. (2019); Di Valentino (2017); Di Valentino et al. (2020, 2021); Perivolaropoulos & Skara (2021); Lucca (2021); Verde et al. (2019); Knox & Millea (2020); Jedamzik et al. (2021); Shah et al. (2021); Abdalla et al. (2022).

The Baryon Acoustic Oscillations (BAO) are sound waves in the baryon-photon plasma comprising the visible matter in the post-inflationary Universe, which froze at recombination epoch. Today, they are observed in the clustering of large-scale structures by numerous galactic surveys (SDSS, DES, WiggleZ, BOSS, etc). Due to rather simple physics of the plasma waves, the BAO can be considered as a standard ruler evolving with the Universe, thus providing another window into studying cosmological models Dunkley et al. (2011); Addison et al. (2013);

Aubourg et al. (2015); Cuesta et al. (2015); Ade et al. (2014b,a); Story et al. (2015); Ade et al. (2016); Alam et al. (2017a); Troxel et al. (2018); Aghanim et al. (2020a); Cuceu et al. (2019); Dainotti et al. (2021). A scale important for BAO measurements is set by the sound horizon at drag epoch. As it is known, at recombination, the photons decouple from the baryons first, at $z_* \approx 1090$, which gives rise to the CMB. The baryons stop feeling the drag of photons at the drag epoch, $z_d \approx 1059$, which sets the standard ruler for the BAO. The Planck Collaboration value of the sound horizon is $r_d^{\text{P18}} = 147.09 \pm 0.26 \text{ Mpc}$ Aghanim et al. (2020a), and the late-time estimation for it is $r_d^{\text{HOLICOW+SN+BAO+SH0ES}} = 136.1 \pm 2.7 \text{ Mpc}$ Arendse et al. (2020). Other estimations give numbers in this range, depending on the datasets in use, for example see Verde et al. (2017); Aghanim et al. (2020b); Alam et al. (2021); Nunes & Bernui (2020); Nunes et al. (2020).

Many papers discuss the relation between the Hubble constant H_0 and the sound horizon scale r_d for different models Aylor et al. (2019); Knox & Millea (2020); Pogossian et al. (2020); Aizpuru et al. (2021). Some claim that resolving the H_0 tension is not enough, since one has to also take into account the model's effect on the sound horizon. This means that one should rule out models that resolve the H_0 tension without resolving the r_d tension simultaneously Jedamzik et al. (2021); Aizpuru et al. (2021); de la Macorra et al. (2021). Since H_0 and r_d are strongly connected, it seems hard to disentangle them without making any assumptions. In order to have an independent cross-check on DE models constraints, we remove the dependence on $H_0 \cdot r_d$ by marginalizing over it using a χ^2 redefinition. Such approach has already been used to different extent in the literature. In Lazkoz et al. (2005) it has been performed on SnIa Gold dataset to compare different parametrizations of $H(z)$. Ref Basilakos & Nesseris (2016) study the growth index by comparing Λ CDM to several dark energy models by marginalizing over M_B and σ_8 . Ref Anagnostopoulos & Basilakos (2018) study differ-

ent cosmological models by marginalizing over H_0 and find that one cannot rule out non-flat models or dynamical dark energy. They observe that the time-varying equation of state parameter $w(z)$ cannot be constrained by the current expansion data. Finally Camarena & Marra (2021) use marginalization over H_0 and M_B in different datasets to show that a hockey-stick dark energy cannot solve the H_0 tension.

One possibility to resolve the tension is by changing the DE model. The question whether the DE is a constant energy density or with a dynamical behavior has been studied in different works Benisty et al. (2021); Capozziello & De Laurentis (2011); Bull et al. (2016); Di Valentino et al. (2021); Yang et al. (2021). This motivates a host of DE parametrizations Wang et al. (2018); Reyes & Escamilla-Rivera (2021); Colgáin et al. (2021); Liu et al. (2021) to be used in the search for deviations from the cosmological constant, Λ , in observational data. A justification for this can be found in numerous papers claiming that DE may resolve the Hubble tension, particularly for the Early Dark Energy models Gogoi et al. (2021); Poulin et al. (2019); Sakstein & Trodden (2020); Tian & Zhu (2021); Nojiri et al. (2021); Seto & Toda (2021); Hill et al. (2022).

In this work, we use two types of datasets for BAO and we combine them with SnIA. Then we marginalize over $H_0 \cdot r_d$ and H_0 and M_B , respectively. This allows us to remove the need of taking priors on these quantities and thus it removes some of the implied assumptions on the models. By this method, we study Λ CDM, wCDM, the CPL parametrization of wwaCDM and also two emergent dark energy models: pEDE and gEDE. We show that even with this more extensive marginalization, one can see differences in the predictions of the different models inferred from the different datasets. The second is particularly interesting in view of the growing sensitivity towards the implied assumptions in processing the data. We then perform a statistical analysis on the so obtained results using 4 well-established measures. We confirm that constraining w_a seems impossible from this method, while the errors on w_0 improve significantly when we add SnIA. Surprisingly, the different BAO datasets show different preference for the flatness of the universe.

The plan of the work is as follows: Section 2 formulates the relevant theory. Section 3 describes the method. Section 4 shows the results with a model comparison. Finally, section 5 summarizes the results.

2. Theory

A Friedmann - Lemaître - Robertson - Walker metric with the scale parameter $a = 1/(1+z)$ is considered, where z is the redshift. The evolution of the Universe for it is governed by the Friedmann equation which connects the equation of the state for Λ CDM background:

$$E(z)^2 = \Omega_m(1+z)^3 + \Omega_K(1+z)^2 + \Omega_\Lambda(z), \quad (1)$$

with the expansion of the Universe $E(z)^2 = H(z)/H_0$, where $H(z) := \dot{a}/a$ is the Hubble parameter at redshift z and H_0 is the Hubble parameter today. Ω_m , Ω_Λ and Ω_K are the fractional densities of matter, DE and the spatial curvature at redshift $z = 0$. We ignore radiation, since we take a look on the late Universe. The spatial curvature is expected to be zero for a flat Universe, $\Omega_K = 0$. We can expand this simple model by considering a DE component depending on z . This can be done with a generalization of the Chevallier-Polarski-Linder (CPL) parametrization Chevallier & Polarski (2001); Linder (2003); Linder & Huterer

(2005); Barger et al. (2006) of the wwaCDM model:

$$\Omega_\Lambda(z) = \Omega_\Lambda^{(0)} \exp \left[\int_0^z \frac{3(1+w(z'))dz'}{1+z'} \right] \quad (2)$$

in which we consider three possible models:

$$w(z) = \begin{cases} w_0 + w_a z & \text{Linear} \\ w_0 + w_a \frac{z}{z+1} & \text{CPL} \\ w_0 - w_a \log(z+1) & \text{Log} \end{cases} \quad (3)$$

which recover Λ CDM for $w_0 = -1$, $w_a = 0$.

To this parametrization we add another model, namely the phenomenologically Emergent Dark Energy (pEDE) Li & Shafieloo (2019, 2020) and its generalization (gEDE). gEDE is described by:

$$\Omega_{DE}(z) = \Omega_\Lambda \frac{1 - \tanh(\bar{\Delta} \log_{10}(\frac{1+z}{1+z_t}))}{1 + \tanh(\bar{\Delta} \log_{10}(1+z_t))} \quad (4)$$

with pEDE-CDM recovered for $\bar{\Delta} = 1$, and Λ CDM for $\bar{\Delta} = 0$. The parameter z_t here is the transitional redshift where $\Omega_{DE}(z_t) = \Omega_m(1+z_t)^3$. Note, z_t is obtained as a solution of this equation and thus, it is not a free parameter, but a calculated one. The analytical form of $w(z)$ then can be obtained from the integral (2), see Li & Shafieloo (2020).

The BAO measurements provide different directions. The radial projection $D_H(z) = c/H(z)$ gives:

$$\frac{D_H}{r_d} = \frac{c}{H_0 r_d} \frac{1}{E(z)}, \quad (5)$$

which includes the parameter $\frac{c}{H_0 r_d}$. The tangential BAO measurements are given in terms of the angular diameter distance D_A :

$$D_A = \frac{c}{H_0 (1+z)} \frac{1}{\sqrt{|\Omega_K|}} \text{sinn} \left[|\Omega_K|^{1/2} \Gamma(z) \right], \quad (6)$$

where $\text{sinn}(x) \equiv \sin(x)$, x , $\sinh(x)$ for $\Omega_K < 0$, $\Omega_K = 0$, $\Omega_K > 0$ respectively. The Γ function is defined as:

$$\Gamma(z) = \int \frac{dz'}{E(z')} \quad (7)$$

where $E(z)$ is related to the equation of state of the Universe as defined above. Thus, the measurement D_A/r_d can expressed as:

$$\frac{D_A}{r_d} = \frac{c}{H_0 r_d} f(z), \quad (8a)$$

where:

$$f(z) = \frac{1}{(1+z) \sqrt{|\Omega_K|}} \text{sinn} \left[|\Omega_K|^{1/2} \Gamma(z) \right]. \quad (8b)$$

A related quantity used in the radial BAO measurements is the comoving angular diameter distance $D_M = D_A(1+z)$.

Furthermore, we use dataset featuring the BAO angular scale measurement $\theta_{BAO}(z)$. It gives the angular diameter distance D_A at the redshift z :

$$\theta_{BAO}(z) = \frac{r_d}{(1+z) D_A(z)} = \frac{H_0 r_d}{c} h(z), \quad (9)$$

with:

$$h(z) = \frac{1}{(1+z)f(z)} \quad (10)$$

z	D_A/r_d	σ_{Data}	year	Ref.
0.11	2.607	0.138	2021	de Carvalho et al. (2021)
0.24	5.594	0.305	2016	Chuang et al. (2017)
0.32	6.636	0.11	2016	Alam et al. (2017b)
0.38	7.389	0.122	2019	Beutler et al. (2017)
0.44	8.19	0.77	2012	Blake et al. (2012)
0.51	7.893	0.279	2015	Carvalho et al. (2016)
0.54	9.212	0.41	2012	Seo et al. (2012)
0.6	9.37	0.65	2012	Blake et al. (2012)
0.697	10.18	0.52	2020	Sridhar et al. (2020); Gil-Marin et al. (2020)*
0.73	10.42	0.73	2012	Blake et al. (2012)
0.81	10.75	0.43	2017	Abbott et al. (2019)
0.85	10.76	0.54	2020	Tamone et al. (2020)
0.874	11.41	0.74	2020	Sridhar et al. (2020)
1.00	11.521	1.032	2019	Zhu et al. (2018)
1.480	12.18	0.32	2020	Hou et al. (2020); Gil-Marin et al. (2020); Bautista et al. (2020)*
2.00	12.011	0.562	2019	Zhu et al. (2018)
2.35	10.83	0.54	2019	Blomqvist et al. (2019), du Mas des Bourboux et al. (2020)*
2.4	10.5	0.34	2017	du Mas des Bourboux et al. (2017)

Table 1. A compilation of BAO measurements from diverse releases of the SDSS, WiggleZ, DES etc. Values marked with * are calculated through their covariance matrices relating D_M and D_H

z	θ	σ_θ	Ref.
0.11	19.80	3.26	de Carvalho et al. (2020)
0.235	9.06	0.23	Alcaniz et al. (2017)
0.365	6.33	0.22	Alcaniz et al. (2017)
0.450	4.77	0.17	Carvalho et al. (2016)
0.470	5.02	0.25	Carvalho et al. (2016)
0.490	4.99	0.21	Carvalho et al. (2016)
0.510	4.81	0.17	Carvalho et al. (2016)
0.530	4.29	0.30	Carvalho et al. (2016)
0.550	4.25	0.25	Carvalho et al. (2016)
0.570	4.59	0.36	Carvalho et al. (2020)
0.590	4.39	0.330	Carvalho et al. (2020)
0.610	3.85	0.31	Carvalho et al. (2020)
0.630	3.90	0.43	Carvalho et al. (2020)
0.650	3.55	0.16	Carvalho et al. (2020)
2.225	1.77	0.31	de Carvalho et al. (2018)

Table 2. A compilation of angular BAO measurements from luminous red and blue galaxies and quasars from diverse releases of the SDSS. The BAO_θ dataset were taken from Nunes et al. (2020).

We see that both D_A/r_d and θ_{BAO} and D_H/r_d depend on the quantity $H_0 \cdot r_d$ which can be eliminated from the corresponding χ^2 , as we demonstrate in the next section.

Finally, we add the type Ia supernovae (SnIA) measurements, described by the luminosity distance $\mu(z)$. It is related to the Hubble parameter through the angular diameter distance as $D_A = d_L(z)/(1+z)^2$. For the SnIA standard candles, the distance modulus $\mu(z)$ is related to the luminosity distance through

$$\mu_B(z) - M_B = 5 \log_{10} [d_L(z)] + 25. \quad (11)$$

where d_L is measured in units of Mpc, and M_B is the absolute magnitude. There is a degeneracy between H_0 and M_B , in such a

way that total absolute magnitude reads: $M_B + 25 + 5 \log_{10} \left(\frac{c/H_0}{Mpc} \right)$. This degeneracy, can also be used to remove the dependence on H_0 and M_B in the χ^2 .

3. Method

In order to infer the parameters of certain model from the observations, one needs to define the appropriate χ^2 . The goal of our analysis is to redefine the corresponding χ^2 in all datasets, in a way that eliminates the dependence on degenerate parameters, such as $H_0 \cdot r_d$ (or H_0 and M_B for SnIA), but maintains the dependence on the equation of state that enter into $\Gamma(z)$.

3.1. BAO redefinition

A DE model includes n-free parameters (i.e. $\Omega_m, \Omega_K, w_0, w_a \dots$), constrained by minimizing the χ^2 :

$$\chi^2 = \sum_i [\mathbf{v}_{obs} - \mathbf{v}_{model}]^T C_{ij}^{-1} [\mathbf{v}_{obs} - \mathbf{v}_{model}] \quad (12)$$

where \mathbf{v}_{obs} is a vector of the observed points at each z (i.e. D_M/r_d , D_H/r_d , D_A/r_d or θ_{BAO}) and \mathbf{v}_{model} is the theoretical prediction of the model. It is possible to rewrite the vector as the dimensionless function multiplied by the $\frac{c}{H_0 r_d}$ parameter:

$$\mathbf{v}_{model} = \frac{c}{H_0 r_d} (f(z), E(z)^{-1}) = \frac{c}{H_0 r_d} \mathbf{f}_{model}. \quad (13)$$

C_{ij} is the covariance matrix. For uncorrelated points the covariance matrix is a diagonal matrix, and its elements are the inverse errors σ_i^{-2} . The statistics of the BAO is not fully a Gaussian but we consider this as an approximation. Following the approach in Lazkoz et al. (2005); Basilakos & Nesseris (2016); Anagnostopoulos & Basilakos (2018); Camarena & Marra (2021), one can isolate $\frac{c}{H_0 r_d}$ in the χ^2 by writing it as:

$$\chi^2 = \left(\frac{c}{H_0 r_d} \right)^2 A - 2B \left(\frac{c}{H_0 r_d} \right) + C, \quad (14)$$

where:

$$A = f^j(z_i) C_{ij} f^i(z_i), \quad (15a)$$

$$B = \frac{f^j(z_i) C_{ij} v_{model}^j(z_i) + v_{model}^j(z_i) C_{ij} f^i(z_i)}{2}, \quad (15b)$$

$$C = v_j^{model} C_{ij} v_i^{model}. \quad (15c)$$

Using Bayes's theorem and marginalizing over $c/(H_0 r_d)$, we arrive at:

$$p(D, M) = \frac{1}{p(D|M)} \int \exp\left[-\frac{1}{2}\chi^2\right] d\frac{c}{H_0 r_d}, \quad (16)$$

where D is the data we use, and the M is the model. Consequently, using $\tilde{\chi}_{BAO}^2 = -2 \ln p(D, M)$ we get the marginalized χ^2 :

$$\tilde{\chi}^2 = C - \frac{B^2}{A} + \log\left(\frac{A}{2\pi}\right), \quad (17)$$

This last equation is the final χ^2 we use. For it, due to the marginalization procedure, the χ^2 depends only on $f(z)$ and $h(z)$ which do not include H_0 and r_d inside.

3.2. θ_{BAO} data

We use the same approach for the $\theta_{BAO}(z)$ measurements:

$$\chi_{\theta, BAO}^2 = \sum_{i=1}^N \left(\frac{\theta(z_i) - \theta_D^i}{\sigma_i} \right)^2, \quad (18)$$

where θ_D^i and σ_i are the observational data and the corresponding uncertainties at the observed redshift z_i . The reconstructed $\chi_{\theta, BAO}^2$, then, is the following:

$$\chi_{\theta, BAO}^2 = \left(\frac{H_0 r_d}{c} \right)^2 A_\theta - 2B_\theta \left(\frac{H_0 r_d}{c} \right) + C, \quad (19)$$

where:

$$A_\theta = \sum_{i=1}^N \frac{h(z_i)^2}{\sigma_i^2}, \quad (20a)$$

$$B_\theta = \sum_{i=1}^N \frac{\theta_D^i h(z_i)}{\sigma_i^2}, \quad (20b)$$

$$C_\theta = \sum_{i=1}^N \frac{(\theta_D^i)^2}{\sigma_i^2}. \quad (20c)$$

Using Bayes's theorem and marginalizing over $H_0 r_d/c$, we arrive at the marginalized χ^2 , which is the same as in Eq (17), only with A , B and C now functions of θ . This $\tilde{\chi}_\theta^2$ also depends only on $h(z)$, without any dependence on $H_0 \cdot r_d/c$.

3.3. Supernova redefinition

Following the approach used in Di Pietro & Claeskens (2003); Nesseris & Perivolaropoulos (2004); Perivolaropoulos (2005); Lazkoz et al. (2005) we assumed no prior constraint on M_B , which is just some constant and we integrated the probabilities over M_B . The integrated χ^2 yields:

$$\tilde{\chi}_{SN}^2 = D - \frac{E^2}{F} + \ln \frac{F}{2\pi}, \quad (21)$$

where:

$$D = \sum_i \left(\frac{\mu^i - 5 \log_{10} [d_L(z_i)]}{\sigma_i} \right)^2, \quad (22a)$$

$$E = \sum_i \frac{\mu^i - 5 \log_{10} [d_L(z_i)]}{\sigma_i^2}, \quad (22b)$$

$$F = \sum_i \frac{1}{\sigma_i^2}. \quad (22c)$$

Here μ^i is the observed luminosity, σ_i is its error and the $d_L(z)$ is the luminosity distance. The values of M and H_0 don't change the marginalized $\tilde{\chi}_{SN}^2$. In order to use the covariance matrix provided for the Pantheon dataset one needs to transform D, E, F as follows:

$$D = \sum_i (\Delta\mu C_{cov}^{-1} \Delta\mu^T)^2, \quad (23a)$$

$$E = \sum_i (\Delta\mu C_{cov}^{-1} E), \quad (23b)$$

$$F = \sum_i C_{cov}^{-1}. \quad (23c)$$

where $\Delta\mu = \mu^i - 5 \log_{10} [d_L(z_i)]$, E is the unit matrix and C_{cov}^{-1} is the inverse covariance matrix of the dataset. The total covariance matrix is given by $C_{cov} = D_{stat} + C_{sys}$, where $D_{stat} = \sigma_i^2$ comes from the measurement and C_{sys} is provided separately Deng & Wei (2018). Notice that the form of $\tilde{\chi}_{BAO}^2$ and $\tilde{\chi}_{SN}^2$ is a bit different, since for the $\tilde{\chi}_{BAO}^2$ we remove the dependence of $c/H_0 r_d$ which multiply the $f(z)$ and in the case of $\tilde{\chi}_{SN}^2$ the parameter \tilde{M} is added the total value of μ .

In our analysis we also consider the combined likelihood

$$\tilde{\chi}^2 = \tilde{\chi}_{BAO}^2 + \tilde{\chi}_{SN}^2. \quad (24)$$

Here $\tilde{\chi}_{BAO}^2$ stands for the BAO or for the BAO_θ datasets independently. The distinction between the hyper-parameters quantifying uncertainties in a dataset and the free parameters of the cosmological model is purely conceptual. It is important to note that the so defined χ^2 is not normalized because of which its absolute value is not a useful measure of the quality of a given fit. Moreover, it is biased towards larger number of parameters and not very good for small datasets, such as the ones we use Lazkoz et al. (2005). For this reason, we use it only to calculate the more balanced statistical measures, see below.

3.4. Datasets and priors

In this work, we consider two different BAO datasets, to which we add the binned Pantheon supernovae dataset with its covariance matrix. The BAO datasets can be found summarized in Table (1) and Table (2).

The first BAO dataset, shown on Table 1 and denoted BAO , contains a combination of various angular measurements, to which we add points from the most recent to date eBOSS data release (DR16), which come as angular (D_M) and radial (D_H) measurements and their covariance. The points and the covariance matrices can be found in Cao & Ratra (2022). This choice of points allows us to integrate the quantity $H_0 \cdot r_d$ by summing the corresponding χ^2 of the two types of measurements. While the covariance for some points is known and we include it, for the rest, we have to additionally test for possible correlations. To do so we use the approach from Kazantzidis & Perivolaropoulos (2018), which we also used in Benisty & Staicova (2021). It consists of adding random correlation terms in the covariance matrix and testing the effect on the final result. Explicitly, we use

$$\sigma_{ii} \rightarrow \sigma_{ii} + \sigma_i \sigma_j / 2,$$

where σ_i is the 1σ error of the points. Applying the procedure shows that the points can be considered "effectively uncorrelated" which allows us to use them to infer the cosmological parameters. Even if there are small correlations, the procedure shows the small correlations don't affect the final result considerably.

The second dataset shown on Table 2, denoted BAO_θ , consists of 15 points, coming from transversal BAO measurements Nunes et al. (2020). Importantly, the transversal BAO analysis does not need to assume a fiducial cosmology, particularly on the Ω_K parameter which is included in the standard BAO analysis Nunes et al. (2020). These points are claimed to be uncorrelated, however, using this cosmology-independent methodology means that their errors are larger than the errors obtained using the standard fiducial cosmology approach. One should note that using a fiducial cosmology is accounted for by the Alcock-Paczynski distortion Lepori et al. (2017), so it does not compromise the integrity of the first dataset. However, we would like to investigate the over-all effect of intrinsic assumptions in the final results and to check if the two datasets are equivalent in this respect.

Finally, we add the Pantheon dataset which contains 1048 supernovae luminosity measurements in the redshift range $z \in (0.01, 2.3)$ Scolnic et al. (2018) binned into 40 points. To the statistical error we add also the systematic errors as provided by the binned covariance matrix¹.

We perform the $H_0 \cdot r_d$ -integration procedure, outlined in previous sections, first on the two different BAO datasets alone, and then on the combination of the appropriate BAO dataset plus the Pantheon dataset. The priors we use are: $\Omega_m \in (0.2, 0.4)$, $w_0 \in (-2, -0)$, $w_a \in (-2, 1)$, $\Omega_K \in (-0.3, 0.3)$. We set $\Omega_\Lambda^{(0)} = 1 - \Omega_m - \Omega_K$. For gEDE we use the redefinition $\Delta = -\tilde{\Delta}$, $w_a = z_t$, so that it can be plotted on the same plots as the other models. As mentioned before z_t is not a free parameter thus it is not a parameter in the MCMC and it is found by solving the appropriate transcendental equation using the package *sympy*. Regarding the problem of likelihood maximization, we use an affine-invariant Markov Chain Monte Carlo (MCMC) nested sampler, as it is implemented within the open-source package *Polychord* Handley et al. (2015) with the *GetDist* package Lewis (2019) to present

the results. In *Polychord* convergence is defined as when the posterior mass contained in the live points is $p = 10^{-2}$ of the total calculated evidence. We check that our chains are stable with respect to changes in the parameter p and furthermore by checking the Geweke score and the Gelmen-Rubin diagnostic with the package *pymcmcstat*.

4. Results

4.1. Posterior Distributions

Figures 1,2,3,4,5 and in the Appendix show the final values obtained by running MCMC on the selected priors for the two different datasets, with the numerical values in the tables II-VI. Since we integrate H_0 and r_d , the only physically measured parameter which remains is Ω_m . We see that in all the cases Ω_m is rather well constrained, even from the BAO-only datasets. The BAO_θ as expected gives larger errors which the inclusion of supernova data improves. The closest to the Planck measurement of $\Omega_m = 0.315 \pm 0.007$ Aghanim et al. (2020b) is the Log model for BAO_θ and the Λ CDM model for BAO , and Λ CDM/OkCDM for $BAO + SN$ and $BAO_\theta + SN$ with the Log model being very close for the latter.

When we consider the other parameters, we see that the BAO only datasets are not able to limit them properly. While the BAO_θ dataset values contain $w_0 = -1$ within 1σ , the values for BAO infer $w_0 > -1$. Adding the SN datasets improves the constraints significantly. With respect to the parameter w_a the inferred values have very big errors. When it comes to Ω_K , BAO_θ gives values closer to a flat universe, while BAO points to $\Omega_K < 0$ (a closed universe).

The two emergent dark energy models perform well in all the cases. pEDE has an error similar to Λ CDM, but at higher Ω_m . gEDE also prefers higher values for Ω_m .

As mentioned in the Theory part, $\Delta = 0$ recovers Λ CDM, while $\Delta = -1$ recovers pEDE. We see from Fig. 4, that Λ CDM is preferred only by BAO , while the other datasets prefer pEDE (i.e. Δ closer to -1) but with large error. On the other hand, z_t is consistent with the known results for $z_t \sim 0.2$. Note that in the tables and in the Appendix, we denote $\Delta \rightarrow w_0$ and $z_t \rightarrow w_a$ for notation consistency with the other models.

The conclusion from our results is that the BAO-alone datasets are useful mostly for constraining Ω_m and to lesser extent w_0 , while they are much less sensitive to the other parameters - w_a or Ω_K . The BAO + SN datasets seem to give much better constraints on the DE parameters. Also, one can see that the BAO_θ dataset includes the Ω_K value of a flat universe, while the BAO dataset seems to exclude it at 68% CL.

From the the Gaussians we see that some DE models have multiple peaks, speaking of some degeneracy. The results do not seem to change with increasing the number of live points, hinting that this is a property of the models themselves or of the selected datasets.

4.2. Model Selection

To compare the different models, we use different well-known statistical measures. We use the Akaike Information Criterion (AIC), and Bayesian Information Criterion (BIC), the Deviance Information Criterion (DIC) and the Bayes Factor (BF) Liddle (2007).

The AIC criterion is defined as:

$$AIC = -2 \ln(\mathcal{L}_{\max}) + 2k + \frac{2k(k+1)}{N_{\text{tot}} - k - 1}, \quad (25)$$

¹ <https://github.com/dscolnic/Pantheon/>

Model	Ω_m	Ω_K	w_0	w_a	ΔAIC	ΔBIC	ΔDIC	$\ln(BF)$
BAO								
LCDM	0.314 ± 0.014	-	-	-	0	0	0	0
wCDM	0.292 ± 0.027	-	-0.658 ± 0.119	-	-1.184	-2.228	0.810	1.693
wwaCDM	0.314 ± 0.053	-	-0.644 ± 0.135	-0.181 ± 0.3	-3.062	-5.151	0.869	0.375
OkLCDM	0.321 ± 0.015	-0.061 ± 0.053	-	-	-3.007	-4.052	-1.216	-0.835
Linear	0.315 ± 0.051	-	-0.63 ± 0.127	-0.196 ± 0.293	-2.995	-5.084	0.930	0.241
CPL	0.293 ± 0.054	-	-0.662 ± 0.173	-0.061 ± 0.606	-3.299	-5.388	0.600	1.267
Log	0.308 ± 0.046	-	-0.651 ± 0.149	0.153 ± 0.376	-3.142	-5.231	0.786	0.639
pEDE	0.31 ± 0.015	-	-	-	0.717	0.717	0.486	-3.796
gEDE	0.311 ± 0.016	-	-0.278 ± 0.209	0.290	-1.728	-2.773	0.161	-1.900
BAO_θ								
LCDM	0.325 ± 0.057	-	-	-	0	0	0	0
wCDM	0.324 ± 0.064	-	-0.929 ± 0.356	-	-1.837	-2.545	0.113	-0.545
wwaCDM	0.319 ± 0.058	-	-0.89 ± 0.43	-0.314 ± 0.73	-3.916	-5.332	0.067	-0.538
OkLCDM	0.327 ± 0.053	0.038 ± 0.181	-	-	-2.075	-2.783	-0.084	0.092
Linear	0.324 ± 0.064	-	-0.872 ± 0.449	-0.337 ± 0.963	-3.821	-5.237	0.118	-0.467
CPL	0.327 ± 0.063	-	-0.854 ± 0.438	-0.448 ± 0.932	-3.791	-5.207	0.141	-0.628
Log	0.316 ± 0.066	-	-1.07 ± 0.432	-0.527 ± 0.97	-3.853	-5.269	0.094	-0.597
pEDE	0.341 ± 0.051	-	-	-	0.165	0.165	0.114	-0.332
gEDE	0.343 ± 0.044	-	-0.877 ± 0.693	0.214	-1.916	-2.624	0.060	-0.184

Table 3. Constraints at 68% CL errors on the cosmological parameters for the different tested models for the two BAO only datasets: *BAO* and *BAO_θ*

Model	Ω_m	Ω_K	w_0	w_a	ΔAIC	ΔBIC	ΔDIC	$\ln(BF)$
BAO + SN								
LCDM	0.305 ± 0.011	-	-	-	0	0	0	0
wCDM	0.302 ± 0.012	-	-0.986 ± 0.045	-	-1.603	-3.714	0.240	-2.777
wwaCDM	0.361 ± 0.034	-	-1.18 ± 0.139	-0.376 ± 0.672	-22.4	-26.6	-18.6	16.9
OkLCDM	0.336 ± 0.018	-0.211 ± 0.066	-	-	-20.9	-23.1	-19.1	18.5
Linear	0.333 ± 0.084	-	-1.128 ± 0.118	-0.125 ± 1.056	-22.4	-26.7	-18.6	16.6
CPL	0.369 ± 0.021	-	-1.166 ± 0.134	-0.569 ± 0.889	-22.2	-26.4	-18.4	16.4
Log	0.335 ± 0.055	-	-1.183 ± 0.111	-0.2 ± 0.865	-22.0	-26.2	-18.2	16.3
pEDE	0.353 ± 0.014	-	-	-	-18.1	-18.1	-18.2	18.4
gEDE	0.36 ± 0.022	-	-1.319 ± 0.478	0.176	-20.3	-22.4	-18.4	18.3
BAO_θ + SN								
LCDM	0.3 ± 0.014	-	-	-	0	0	0	0
wCDM	0.321 ± 0.049	-	-1.084 ± 0.141	-	-1.765	-3.772	0.144	-1.650
wwaCDM	0.338 ± 0.044	-	-1.095 ± 0.091	-0.311 ± 0.739	-3.978	-7.992	-0.068	-1.742
OkLCDM	0.312 ± 0.027	-0.089 ± 0.147	-	-	-1.918	-3.926	0.014	-0.229
Linear	0.33 ± 0.061	-	-1.072 ± 0.117	-0.279 ± 0.817	-3.739	-7.753	0.119	-2.107
CPL	0.332 ± 0.052	-	-1.071 ± 0.124	-0.344 ± 0.922	-3.707	-7.721	0.213	-1.901
Log	0.318 ± 0.062	-	-1.087 ± 0.126	-0.027 ± 0.653	-3.794	-7.808	0.052	-1.763
pEDE	0.348 ± 0.014	-	-	-	-0.037	-0.037	-0.061	-0.120
gEDE	0.339 ± 0.027	-	-0.892 ± 0.64	0.219	-2.047	-4.055	0.015	0.062

Table 4. Constraints at 68% CL errors on the cosmological parameters for the different tested models for the two BAO + SN datasets: *BAO + SN* and *BAO_θ + SN*

where \mathcal{L}_{\max} is the maximum likelihood of the data under consideration and N_{tot} is the total number of data points and k is the number of parameters. For large N_{tot} , this expression reduces to $AIC \approx -2 \ln(\mathcal{L}_{\max}) + 2k$, which is the standard form of the AIC criterion Liddle (2007).

The BIC criterion is an estimator of the Bayesian evidence, (e. g Liddle (2007)), and is given as

The AIC and BIC criteria employ only the likelihood value at maximum. Since we evaluate this \mathcal{L}_{\max} numerically, from the Bayesian analysis, one needs to use sufficiently long chains to ensure the accuracy of \mathcal{L}_{\max} when evaluating AIC and BIC. The Deviance Information Criterion (DIC) Liddle (2007) provides all the information obtained from the likelihood calls during the maximization procedure. The DIC estimator is defined as,

$$BIC = -2 \ln(\mathcal{L}_{\max}) + k \log(N_{\text{tot}}).$$

$$(26) \quad DIC = 2\overline{D(\theta)} - D(\bar{\theta})$$

$$(27)$$

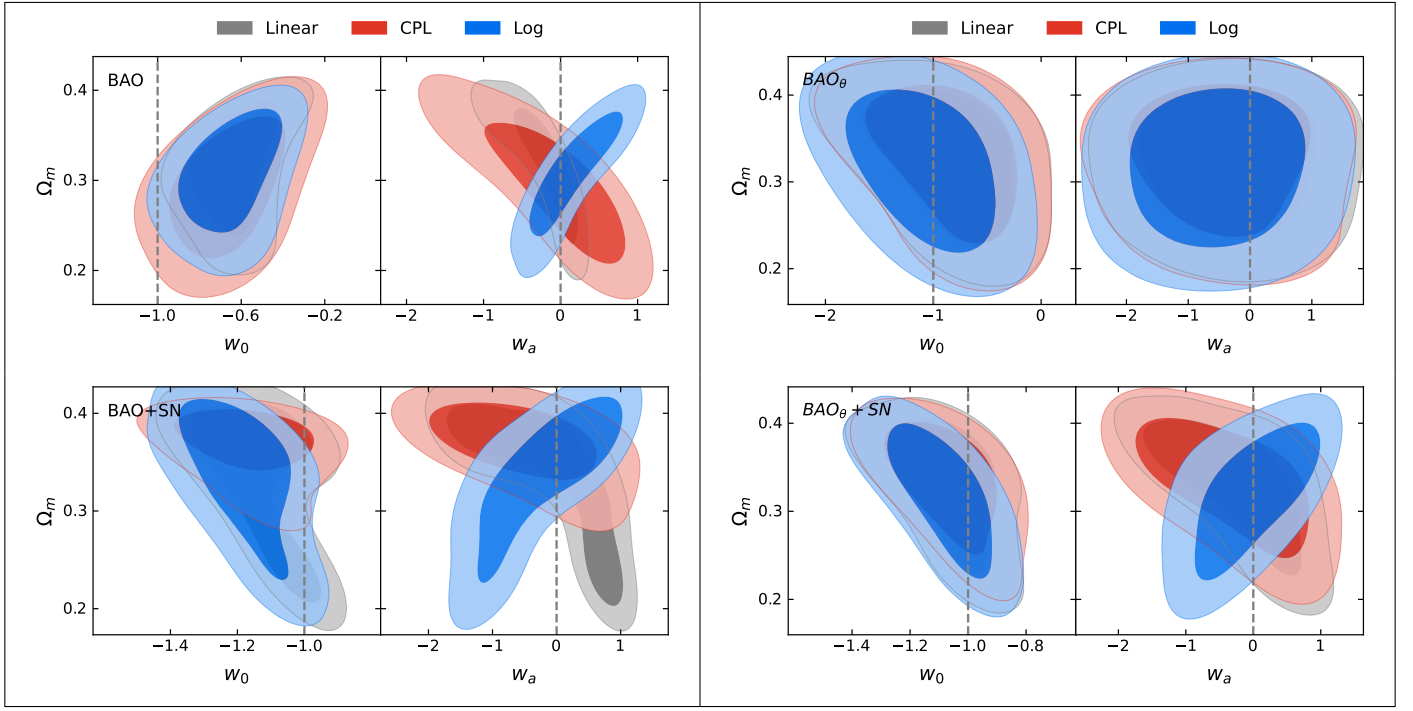


Fig. 1. The posterior distribution for Ω_m and w_0, w_a for different parametrizations of the w waCDM model with the BAO and BAO_θ datasets to the left and to the right, and with the Pantheon data added to the bottom panel

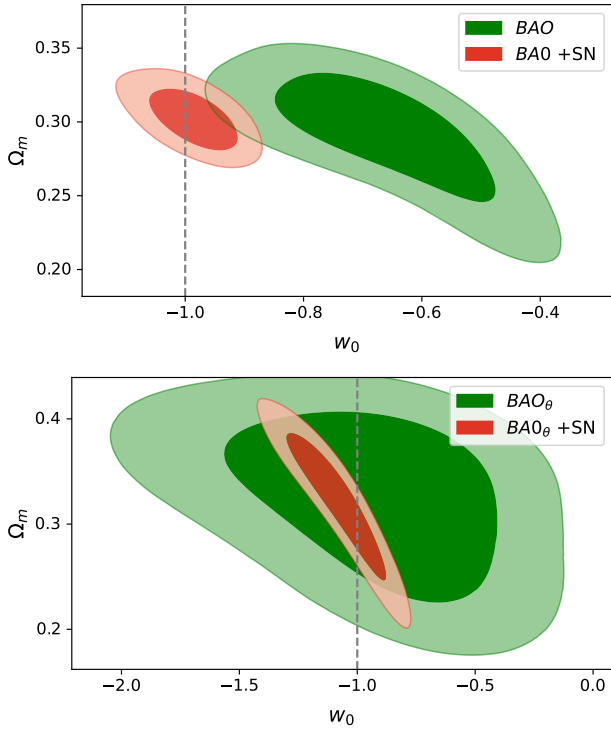


Fig. 2. The posterior distribution for Ω_m and w_0 for the w CDM model with the BAO data on the upper and the BAO_θ data to the lower

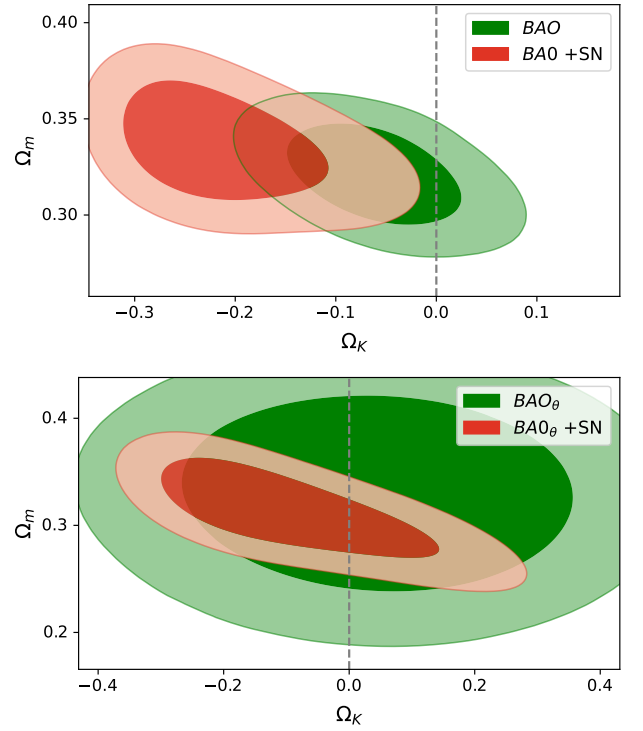


Fig. 3. The posterior distribution for Ω_m and Ω_k for Ω_k LCDM model with the BAO data on the upper and the BAO_θ data to the lower

where θ is the vector of parameters being varied in the model, the overline denotes the usual mean value and $D(\theta) = -2 \ln(\mathcal{L}(\theta)) + C$, where C is a constant. We use these definitions to form the difference in the IC values of the default model (Λ CDM) and the other suggested models. I.e. we calculate $\Delta IC_{\text{model}} = IC_{\Lambda\text{CDM}} - IC_{\text{model}}$. The model with the minimal AIC is consid-

ered best, Jeffreys (1939), so a positive ΔIC will point to a preference towards the DE model, negative – towards Λ CDM with $|\Delta IC| \geq 2$ signifying a possible tension, $|\Delta IC| \geq 6$ – a medium tension, $\Delta IC \geq 10$ – a strong tension. Finally we use the Bayes

factor, defined as:

$$B_{ij} = \frac{p(d|M_i)}{p(d|M_j)}$$

where $p(d|M_i)$ is the Bayesian evidence for model M_i . The evidence is difficult to calculate analytically, but in polychord, it is calculated numerically by the algorithm. In the tables below, we use the $\ln(B_{0i})$ where "0" is Λ CDM, which we compare with all the other models (denoted by the index "i"). According to the Jeffery's scale Jeffreys (1939), $\ln(B_{ij}) < 1$ is inconclusive for any of the models, 1-2.5 gives weak support for the model "i", 2.5 to 5 is moderate and > 5 is strong evidence for the model "i". A minus sign gives the same for model "j".

The so defined statistical measures for the two datasets are presented in tables 3 and 4. In summary, the model comparison for the different datasets gives:

- For the *BAO* dataset: the best model from AIC, BIC and DIC is Λ CDM, followed closely (within < 1 IC units) by pEDE. The BF agrees on that, with pEDE and gEDE being close to it. OkLCDM is comparable to LCDM.
- For the *BAO + SN* dataset: the best model is Λ CDM from all IC measures. BF agrees with that for most models, with inconclusive preference for wCDM ($\ln(BF) < -1$).
- For the *BAO _{θ}* dataset, the best model for AIC and BIC is pEDE followed by Λ CDM. For DIC the best model is CPL, with all wCDM and wwaCDM models being better than Λ CDM. The IC difference, however, is too small to signify any tension. The BF agrees with DIC, with CPL model being best, Λ CDM - the worst. Again, inconclusively.
- For the *BAO _{θ}* + SN dataset, with respect to the AIC and BIC, the best model is Λ CDM, but pEDE is very close to it. With respect to DIC, all the models give better results than Λ CDM, with CPL - best, but the statistical significance is extremely low. With respect to BF, however, the 3 parametrizations of wwaCDM give best results, with values representing a weak but non-negligible support.

From this comparison we see that first, the use of statistical measures does not give entirely consistent view on the selecting the best model. This can be due to a number of factors - slow convergence of some of the models, priors not having the similar weight etc.

Second, the two BAO datasets have preferences for different models. This may be due to different intrinsic assumptions with which the measurements have been made. The *BAO _{θ}* dataset, despite the larger errors, seems to give consistent results, with some weak support for DE models in the different measures. The more standard AIC and BIC, however, are always in favor of Λ CDM, with pEDE being close behind. The *BAO* dataset seems to always prefer Λ CDM in most measures.

We can conclude that from the two datasets of BAO points, only the *BAO* dataset has a strong preference for Λ CDM. Adding the Pantheon dataset to it boosts this preference to statistical significance. The fact that Λ CDM is not the best model statistically in all of the cases for the BAO-only datasets, may be due to the big uncertainty related to the BAO measurement or the specifics of the chosen dataset. While including the Pantheon dataset decreases the deviation in general, it does not eliminate it entirely for *BAO _{θ}* . This could be due to the different redshift distributions of BAO and Pantheon affecting the model fit: the maximum redshift for the binned Pantheon is $z_{max}^{SN} = 1.6$ vs $z_{max}^{BAO} = 2.4$ for BAO, and the median redshifts are accordingly $\bar{z}^{SN} = 0.2$ vs $\bar{z}^{BAO} = 0.6$. Taking into consideration the big errors of the DE parameters for the different models and that all the evidences

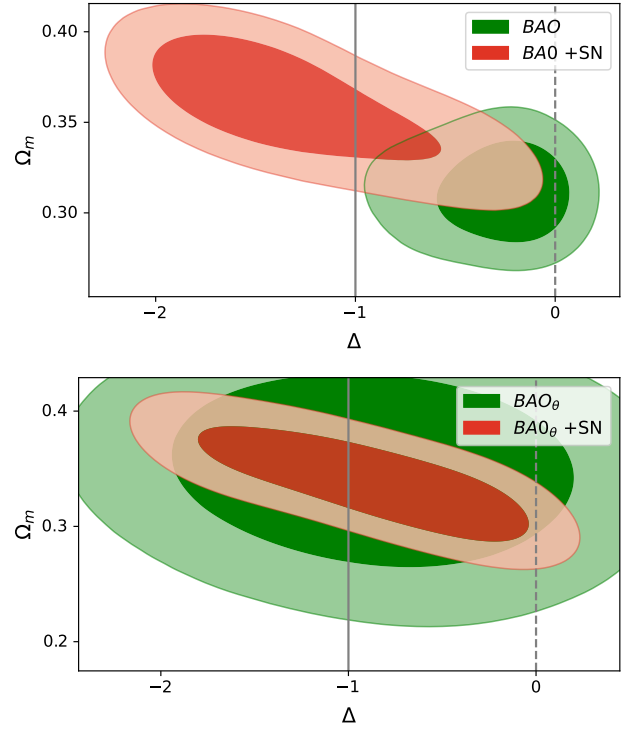


Fig. 4. The posterior distribution for Ω_m and Δ in the gEDE model with the BAO data to the upper panel and the *BAO _{θ}* data to the lower, with the solid line corresponding to pEDE and the dashed line to Λ CDM

against Λ CDM are weak, we see that one needs much better BAO data to get a statistically strong preference if there is such.

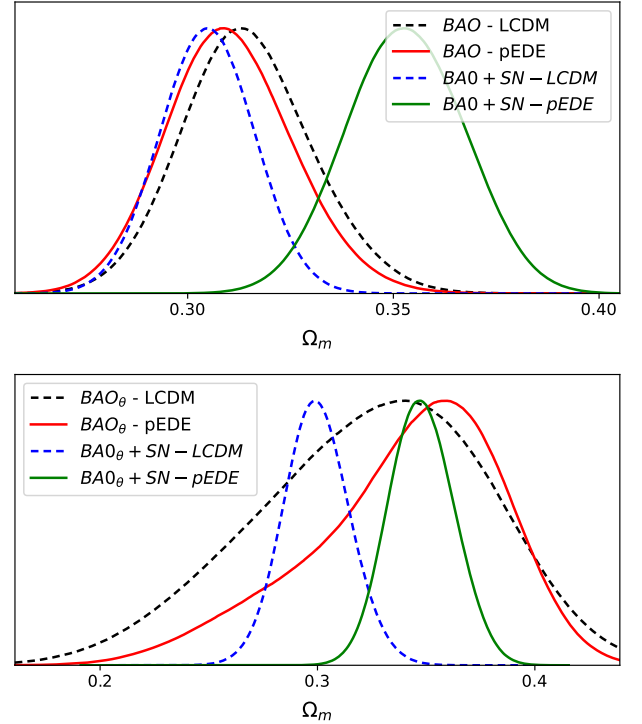


Fig. 5. The posterior distribution for Ω_m for the two 1-parameter models: LCDM and pEDE for the BAO and *BAO _{θ}* datasets

5. Discussion

In order to avoid the problem of the degeneracy between $H_0 - r_d$ in the BAO measurements, and the assumptions on the data it imposes, this paper removes the combination $H_0 \cdot r_d$ entirely by marginalizing over it in the χ^2 . We use two different BAO datasets to test our approach. The first one – named *BAO* comes from different measurement provided by SDSS, WiggleZ, DES etc., in addition to radial measurements coming from DR16 with their covariances. The other dataset is the *BAO_θ* compilation measuring $\theta(z)$, which is based on angular BAO measurements obtained from analyses of luminous red galaxies, blue galaxies, and quasars. These transversal BAO data has the advantage to be weakly dependent on the cosmological model. Both D_A/r_d , D_M/r_d and D_H/r_d provided from the first dataset and $\theta(z)$, provided from the second one, depend only on the combination $H_0 \cdot r_d$ which we integrate out. In a similar way, one can integrate out the dependence on H_0 and M_B in the Pantheon SNIa dataset, leaving all the the likelihoods depending purely on the equation of state, i.e. Ω_m and the DE parameters Ω_Λ , w_0 and w_a , which allows us to use these datasets to infer the corresponding cosmological parameters.

We find that the BAO only datasets infer very well Ω_m , close to the expected values and with a small error, but they are not sufficient to constrain significantly the parameters of the DE models. The errors on w_0 and particularly on w_a are significant within the rather wide priors we use. The errors for the *BAO_θ* dataset are larger than the errors of the *BAO* dataset as expected.

Adding the Type Ia supernova reduces the errors, especially for the w_0 parameter. For the *BAO + SN* dataset, we find $w = -0.986 \pm 0.045$. For $w_{w_a}\text{CDM}$ we find $w_0 = -1.18 \pm 0.139$, $w_a = -0.376 \pm 0.672$. From the *BAO_θ + SN* dataset, we find $w = -1.08 \pm 0.14$ for the $w\text{CDM}$ model. For $w_{w_a}\text{CDM}$ we find $w_0 = -1.09 \pm 0.09$, $w_a = -0.31 \pm 0.74$. As for the curvature, *BAO + SN* dataset prefers a closed, almost flat, universe ($\Omega_k = -0.21 \pm 0.07$), while *BAO_θ + SN* dataset prefers a flat one ($\Omega_k = -0.09 \pm 0.15$). In both cases, the gEDE model is closer to pEDE than to ΛCDM .

Comparing to the SDSS-IV results Alam et al. (2021), we see that they predict $w_0 = -0.939 \pm 0.073$, $w_a = -0.31 \pm 0.3$ when one considers BAO+SN+CMB, but $w_0 = -0.69 \pm 0.15$ when only the BAO dataset is used. Thus our results are consistent in both cases, with the BAO+SN value for w_0 a little lower and the BAO only value - very close to theirs. The mean value for w_a is close, but with much larger error. But we see that in SDSS-IV results, the error on w_a is also rather large. Our results also predict a negative Ω_k , with larger error. One should note, however, that while we include some of the most recent BAO measurements, we include only the angular part of DR12, due to its inter-redshift covariance. Also, the *BAO_θ* datasets has larger inherent errors thus it is expected to lead to larger errors in the inferred parameters. Finally, under the procedure we apply, some precision is lost due to the marginalization itself. Taking into account all this, we see that the procedure we employ still gives results close to the expected.

We perform a number of statistical tests for model comparison. The two BAO datasets show small statistical preferences for different models: ΛCDM for the *BAO* dataset and DE ($w_{w_a}\text{CDM}$, but also pEDE/gEDE) for the *BAO_θ* dataset. When we add the SN dataset, ΛCDM remains the best model for *BAO + SN* dataset, but the *BAO_θ + SN* dataset shows weak but non-negligible preference for DE models.

Our conclusion is that one cannot constrain sufficiently the DE models from the chosen uncalibrated, mostly angular, BAO

datasets alone. Adding the Type Ia supernova to further reduce the errors and to remove some possible degeneracy helps but it only helps to constrain w_0 and not so much w_a . However, the results on Ω_m and w_0 seem constrained enough to confirm the usefulness of this new approach. A downside is that for the moment, it is not possible to include all correlated $D_M - D_H$ measurements, since it is not possible to integrate out $H_0 \cdot r_d$ for a covariance matrix over different z . For this reason we have not used all known correlations in the BAO data which will improve on the errors and thus could lead to better constraints. We predict that future measurements of the BAO would increase the efficiency of the approach as long as the correlation between some redshifts is not large. In any case, the marginalization approach offers a new perspective on the degeneracy $H_0 - r_d - \Omega_m$ since in this case, the only varying parameter is Ω_m and it could be a tool for an independent crosscheck on DE models.

Acknowledgements. We thank Eleonora Di-Valentino and Sunny Vagnozzi for useful comments and discussions. We would like to also thank the anonymous referee for their helpful comments regarding the manuscript. D.B. thanks to the Grants Committee of the Rothschild and the Blavatnik Cambridge Fellowships for generous supports. D.B. acknowledges a Postdoctoral Research Associationship at the Queens' College, University of Cambridge. D.B. & D.S. is thankful to Bulgarian National Science Fund for support via research grant KP-06-N 58/5. We have received partial support from European COST actions CA15117 and CA18108.

References

- Abbott, T. M. C. et al. 2019, Mon. Not. Roy. Astron. Soc., 483, 4866
 Abdalla, E. et al. 2022, JHEAp, 34, 49
 Addison, G. E., Hinshaw, G., & Halpern, M. 2013, Mon. Not. Roy. Astron. Soc., 436, 1674
 Ade, P. A. R. et al. 2014a, Phys. Rev. Lett., 113, 021301
 Ade, P. A. R. et al. 2014b, Astron. Astrophys., 571, A16
 Ade, P. A. R. et al. 2016, Astron. Astrophys., 594, A13
 Aghanim, N. et al. 2020a, Astron. Astrophys., 641, A6, [Erratum: Astron. Astrophys. 652, C4 (2021)]
 Aghanim, N. et al. 2020b, Astron. Astrophys., 641, A6
 Aizpuru, A., Arjona, R., & Nesseris, S. 2021, Phys. Rev. D, 104, 043521
 Alam, S. et al. 2017a, Mon. Not. Roy. Astron. Soc., 470, 2617
 Alam, S. et al. 2017b, Mon. Not. Roy. Astron. Soc., 470, 2617
 Alam, S. et al. 2021, Phys. Rev. D, 103, 083533
 Alcaniz, J. S., Carvalho, G. C., Bernui, A., Carvalho, J. C., & Benetti, M. 2017, Fundam. Theor. Phys., 187, 11
 Anagnostopoulos, F. K. & Basilakos, S. 2018, Phys. Rev. D, 97, 063503
 Arendse, N. et al. 2020, Astron. Astrophys., 639, A57
 Aubourg, E. et al. 2015, Phys. Rev. D, 92, 123516
 Aylor, K., Joy, M., Knox, L., et al. 2019, Astrophys. J., 874, 4
 Barger, V., Guarnaccia, E., & Marfatia, D. 2006, Phys. Lett. B, 635, 61
 Basilakos, S. & Nesseris, S. 2016, Phys. Rev. D, 94, 123525
 Bautista, J. E. et al. 2020, Mon. Not. Roy. Astron. Soc., 500, 736
 Benisty, D. & Staicova, D. 2021, Astron. Astrophys., 647, A38
 Benisty, D., Vasak, D., Kirsch, J., & Struckmeier, J. 2021, Eur. Phys. J. C, 81, 125
 Beutler, F. et al. 2017, Mon. Not. Roy. Astron. Soc., 464, 3409
 Blake, C. et al. 2012, Mon. Not. Roy. Astron. Soc., 425, 405
 Blomqvist, M. et al. 2019, Astron. Astrophys., 629, A86
 Bull, P. et al. 2016, Phys. Dark Univ., 12, 56
 Camarena, D. & Marra, V. 2021, Mon. Not. Roy. Astron. Soc., 504, 5164
 Cao, S. & Ratra, B. 2022, Mon. Not. Roy. Astron. Soc., 513, 5686
 Capozziello, S. & De Laurentis, M. 2011, Phys. Rept., 509, 167
 Carvalho, G. C., Bernui, A., Benetti, M., Carvalho, J. C., & Alcaniz, J. S. 2016, Phys. Rev. D, 93, 023530
 Carvalho, G. C., Bernui, A., Benetti, M., et al. 2020, Astropart. Phys., 119, 102432
 Chevallier, M. & Polarski, D. 2001, Int. J. Mod. Phys. D, 10, 213
 Chuang, C.-H. et al. 2017, Mon. Not. Roy. Astron. Soc., 471, 2370
 Colgáin, E., Sheikh-Jabbari, M. M., & Yin, L. 2021 [arXiv:2104.01930]
 Cuceu, A., Farr, J., Lemos, P., & Font-Ribera, A. 2019, JCAP, 10, 044
 Cuesta, A. J., Verde, L., Riess, A., & Jimenez, R. 2015, Mon. Not. Roy. Astron. Soc., 448, 3463
 Dainotti, M. G., De Simone, B., Schiavone, T., et al. 2021, Astrophys. J., 912, 150

- de Carvalho, E., Bernui, A., Avila, F., Novaes, C. P., & Nogueira-Cavalcante, J. P. 2021, *Astron. Astrophys.*, 649, A20
- de Carvalho, E., Bernui, A., Carvalho, G. C., Novaes, C. P., & Xavier, H. S. 2018, *JCAP*, 04, 064
- de Carvalho, E., Bernui, A., Xavier, H. S., & Novaes, C. P. 2020, *Mon. Not. Roy. Astron. Soc.*, 492, 4469
- de la Macorra, A., Almaraz, E., & Garrido, J. 2021 [arXiv:2106.12116]
- Deng, H.-K. & Wei, H. 2018, *Eur. Phys. J. C*, 78, 755
- Di Pietro, E. & Claeskens, J.-F. 2003, *Mon. Not. Roy. Astron. Soc.*, 341, 1299
- Di Valentino, E. 2017, *Nature Astron.*, 1, 569
- Di Valentino, E., Mena, O., Pan, S., et al. 2021 [arXiv:2103.01183]
- Di Valentino, E. et al. 2020 [arXiv:2008.11284]
- du Mas des Bourboux, H. et al. 2017, *Astron. Astrophys.*, 608, A130
- du Mas des Bourboux, H. et al. 2020, *Astrophys. J.*, 901, 153
- Dunkley, J. et al. 2011, *Astrophys. J.*, 739, 52
- Freedman, W. L. & Madore, B. F. 2010, *Ann. Rev. Astron. Astrophys.*, 48, 673
- Freedman, W. L. et al. 2001, *Astrophys. J.*, 553, 47
- Gil-Marín, H. et al. 2020, *Mon. Not. Roy. Astron. Soc.*, 498, 2492
- Gogoi, A., Sharma, R. K., Chanda, P., & Das, S. 2021, *Astrophys. J.*, 915, 132
- Handley, W. J., Hobson, M. P., & Lasenby, A. N. 2015, *Mon. Not. Roy. Astron. Soc.*, 450, L61
- Hill, J. C. et al. 2022, *Phys. Rev. D*, 105, 123536
- Hou, J. et al. 2020, *Mon. Not. Roy. Astron. Soc.*, 500, 1201
- Jedamzik, K., Pogossian, L., & Zhao, G.-B. 2021, *Commun. in Phys.*, 4, 123
- Jeffreys, H. 1939, *The Theory of Probability*, Oxford Classic Texts in the Physical Sciences
- Kazantzidis, L. & Perivolaropoulos, L. 2018, *Phys. Rev. D*, 97, 103503
- Knox, L. & Millea, M. 2020, *Phys. Rev. D*, 101, 043533
- Lazkoz, R., Nesseris, S., & Perivolaropoulos, L. 2005, *JCAP*, 11, 010
- Lepori, F., Di Dio, E., Viel, M., Baccigalupi, C., & Durrer, R. 2017, *JCAP*, 02, 020
- Lewis, A. 2019 [arXiv:1910.13970]
- Li, X. & Shafieloo, A. 2019, *Astrophys. J. Lett.*, 883, L3
- Li, X. & Shafieloo, A. 2020, *Astrophys. J.*, 902, 58
- Liddle, A. R. 2007, *Mon. Not. Roy. Astron. Soc.*, 377, L74
- Linder, E. V. 2003, *Phys. Rev. Lett.*, 90, 091301
- Linder, E. V. & Huterer, D. 2005, *Phys. Rev. D*, 72, 043509
- Liu, W., Anchordoqui, L. A., Di Valentino, E., et al. 2021 [arXiv:2108.04188]
- Lucca, M. 2021 [arXiv:2105.09249]
- Nesseris, S. & Perivolaropoulos, L. 2004, *Phys. Rev. D*, 70, 043531
- Nojiri, S., Odintsov, S. D., Saez-Chillon Gomez, D., & Sharov, G. S. 2021 [arXiv:2103.05304]
- Nunes, R. C. & Bernui, A. 2020, *Eur. Phys. J. C*, 80, 1025
- Nunes, R. C., Yadav, S. K., Jesus, J. F., & Bernui, A. 2020, *Mon. Not. Roy. Astron. Soc.*, 497, 2133
- Perivolaropoulos, L. 2005, *Phys. Rev. D*, 71, 063503
- Perivolaropoulos, L. & Skara, F. 2021 [arXiv:2105.05208]
- Perlmutter, S. et al. 1999, *Astrophys. J.*, 517, 565
- Pogossian, L., Zhao, G.-B., & Jedamzik, K. 2020, *Astrophys. J. Lett.*, 904, L17
- Poulin, V., Smith, T. L., Karwal, T., & Kamionkowski, M. 2019, *Phys. Rev. Lett.*, 122, 221301
- Reyes, M. & Escamilla-Rivera, C. 2021 [arXiv:2104.04484]
- Riess, A. G., Breuval, L., Yuan, W., et al. 2022a [arXiv:2208.01045]
- Riess, A. G., Casertano, S., Yuan, W., et al. 2021, *Astrophys. J. Lett.*, 908, L6
- Riess, A. G. et al. 1998, *Astron. J.*, 116, 1009
- Riess, A. G. et al. 2016, *Astrophys. J.*, 826, 56
- Riess, A. G. et al. 2022b, *Astrophys. J. Lett.*, 934, L7
- Sakstein, J. & Trodden, M. 2020, *Phys. Rev. Lett.*, 124, 161301
- Schöneberg, N., Lesgourgues, J., & Hooper, D. C. 2019, *JCAP*, 10, 029
- Scolnic, D. M. et al. 2018, *Astrophys. J.*, 859, 101
- Seo, H.-J. et al. 2012, *Astrophys. J.*, 761, 13
- Seto, O. & Toda, Y. 2021, *Phys. Rev. D*, 103, 123501
- Shah, P., Lemos, P., & Lahav, O. 2021, *Astron. Astrophys. Rev.*, 29, 9
- Sridhar, S., Song, Y.-S., Ross, A. J., et al. 2020, *Astrophys. J.*, 904, 69
- Story, K. T. et al. 2015, *Astrophys. J.*, 810, 50
- Tamone, A. et al. 2020, *Mon. Not. Roy. Astron. Soc.*, 499, 5527
- Tian, S. X. & Zhu, Z.-H. 2021, *Phys. Rev.*, D103, 043518
- Troxel, M. A. et al. 2018, *Phys. Rev. D*, 98, 043528
- Verde, L., Bernal, J. L., Heavens, A. F., & Jimenez, R. 2017, *Mon. Not. Roy. Astron. Soc.*, 467, 731
- Verde, L., Treu, T., & Riess, A. G. 2019, *Nature Astron.*, 3, 891
- Wang, Y., Pogossian, L., Zhao, G.-B., & Zucca, A. 2018, *Astrophys. J. Lett.*, 869, L8
- Yang, W., Di Valentino, E., Pan, S., Wu, Y., & Lu, J. 2021, *Mon. Not. Roy. Astron. Soc.*, 501, 5845
- Zhu, F. et al. 2018, *Mon. Not. Roy. Astron. Soc.*, 480, 1096

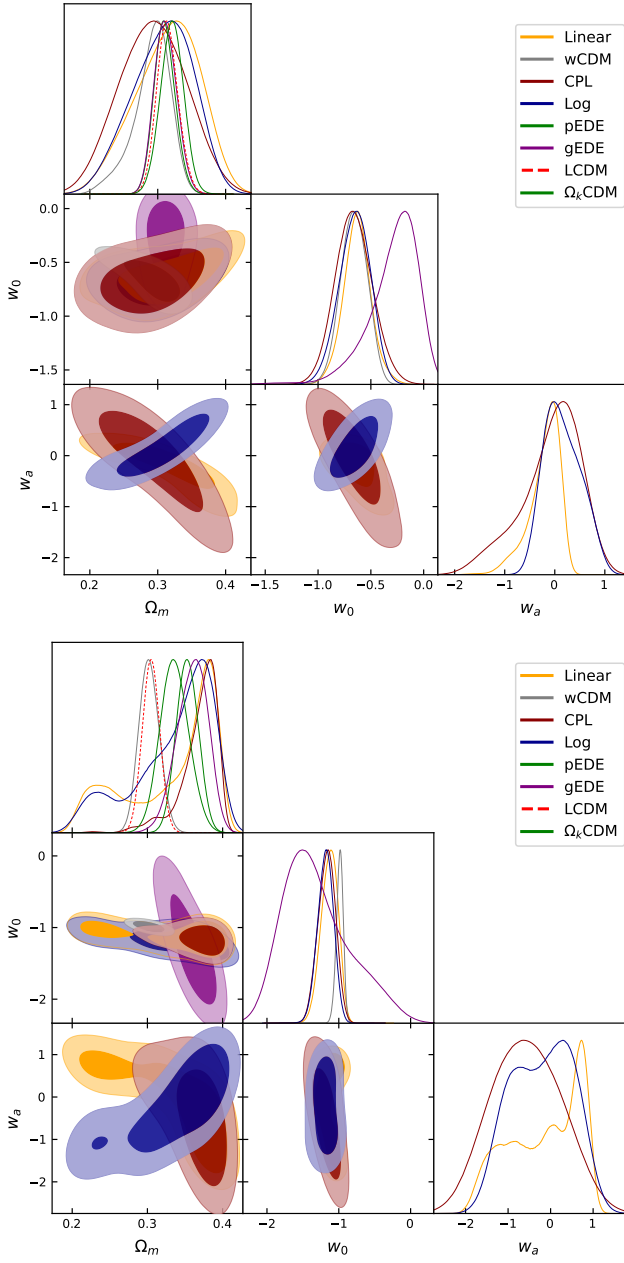


Fig. .1. The posterior distribution for Ω_m and w_0, w_a for different parametrization of DE with the BAO data only on the upper and the combined BAO + Pantheon data to the lower

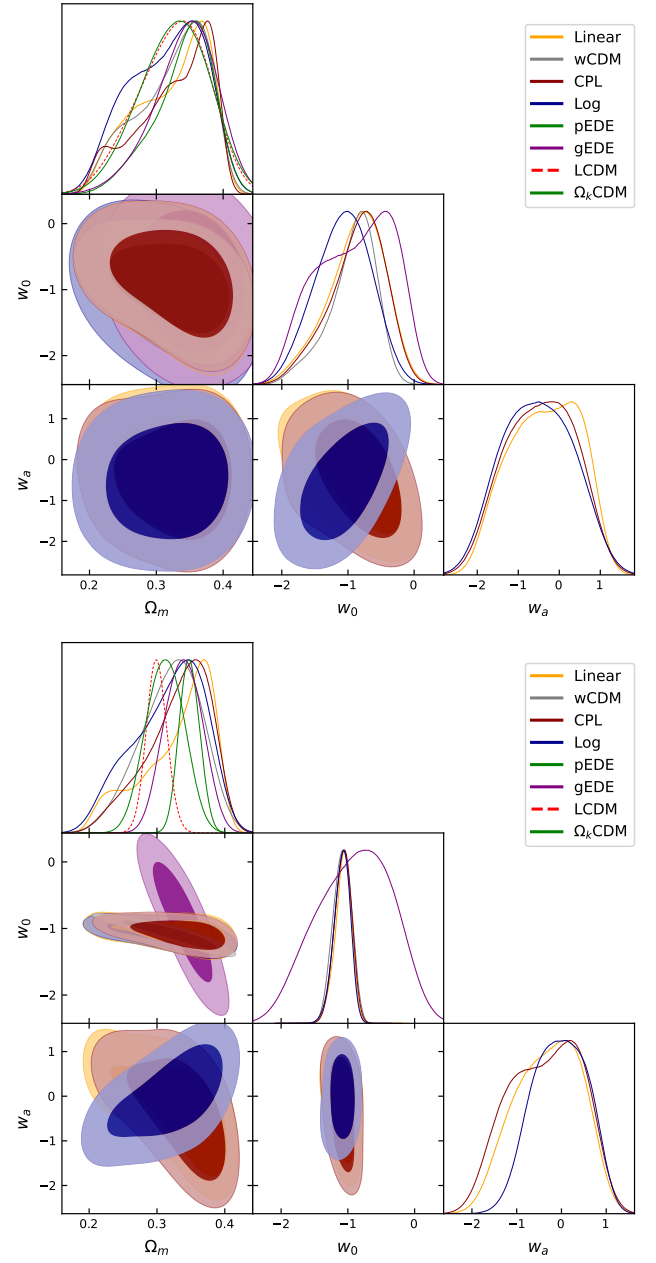


Fig. .2. The posterior distribution for Ω_m and w_0, w_a for different parametrization of DE with the BAO_0 data only on the upper and the combined BAO_0 + Pantheon data to the lower.